

Self-assembly behavior of thermoresponsive difunctionalized γ -amide polycaprolactone amphiphilic diblock copolymers

Hanghang Wang^a, Erika L. Calubaquib^a, Abhi Bhadran^a, Ziyuan Ma^a, Justin T. Miller^a, Anyue Zhang^a, Michael C. Biewer^a, and Mihaela C. Stefan^{*a}

^a Department of Chemistry and Biochemistry, University of Texas at Dallas, Richardson, TX, USA

* Correspondence to Mihaela C Stefan at mihaela@utdallas.edu

Supporting Information

Fig. S1. ¹H NMR spectrum of the intermediate compound *N*-(2-(2-(2-methoxyethoxy)ethoxy)ethyl)propan-1-amine.

Fig. S2. ¹³C NMR spectrum of the intermediate compound *N*-(2-(2-(2-methoxyethoxy)ethoxy)ethyl)propan-1-amine.

Fig. S3. ¹H NMR spectrum of the intermediate compound *N*-propyl-*N*-(2-(2-(2-methoxyethoxy)ethoxy)ethyl)-4-oxocyclohexane-1-carboxamide.

Fig. S4. ¹³C NMR spectrum of the intermediate compound *N*-propyl-*N*-(2-(2-(2-methoxyethoxy)ethoxy)ethyl)-4-oxocyclohexane-1-carboxamide.

Fig. S5. ¹H NMR spectrum of monomer *N*-propyl-*N*-(2-(2-(2-methoxyethoxy)ethoxy)ethyl)-7-oxoxepane-4-carboxamide (γ -ME₃PyCL).

Fig. S6. ¹³C NMR spectrum of monomer *N*-propyl-*N*-(2-(2-(2-methoxyethoxy)ethoxy)ethyl)-7-oxoxepane-4-carboxamide (γ -ME₃PyCL).

Fig. S7. MALDI-ToF mass spectrum of monomer *N*-propyl-*N*-(2-(2-(2-methoxyethoxy)ethoxy)ethyl)-7-oxoxepane-4-carboxamide (γ -ME₃PyCL).

Fig. S8. ¹H NMR spectrum of the homopolymer PME₃PyCL.

Fig. S9. ¹³C NMR spectrum of the homopolymer PME₃PyCL.

Fig. S10. ¹H NMR spectrum of the amphiphilic diblock copolymer poly(γ -benzyloxy- ϵ -caprolactone)-*b*-poly(*N*-propyl-*N*-(2-(2-(2-methoxyethoxy)ethoxy)ethyl)-7-oxoxepane-4-carboxamide) (PBnCL-*b*-PME₃PyCL).

Fig. S11. ¹³C NMR spectrum of the amphiphilic diblock copolymer poly(γ -benzyloxy- ϵ -caprolactone)-*b*-poly(*N*-propyl-*N*-(2-(2-(2-methoxyethoxy)ethoxy)ethyl)-7-oxoxepane-4-carboxamide) (PBnCL-*b*-PME₃PyCL).

Fig. S12. ¹H NMR spectrum of the amphiphilic diblock copolymer polycaprolactone-*b*-poly(*N*-propyl-*N*-(2-(2-(2-methoxyethoxy)ethoxy)ethyl)-7-oxoxepane-4-carboxamide) (PCL-*b*-PME₃PyCL).

Fig. S13. ¹³C NMR spectrum of the amphiphilic diblock copolymer polycaprolactone-*b*-poly(*N*-propyl-*N*-(2-(2-(2-methoxyethoxy)ethoxy)ethyl)-7-oxoxepane-4-carboxamide) (PCL-*b*-PME₃PyCL).

Fig. S14. ^1H NMR spectrum of the amphiphilic diblock copolymer polycaprolactone-*b*-poly(γ -2-(2-(2-methoxyethoxy)ethoxy)ethoxy- ϵ -caprolactone) (PCL-*b*-PME₃CL).

Fig. S15. ^{13}C NMR spectrum of the amphiphilic diblock copolymer polycaprolactone-*b*-poly(γ -2-(2-(2-methoxyethoxy)ethoxy)ethoxy- ϵ -caprolactone) (PCL-*b*-PME₃CL).

Fig. S16. Size exclusion chromatography (SEC) of homopolymer PME₃PyCL and amphiphilic diblock copolymers PBnCL-*b*-PME₃PyCL, PCL-*b*-PME₃PyCL, and PCL-*b*-PME₃CL.

Fig. S17. Differential scanning calorimetry (DSC) of homopolymer PME₃PyCL and amphiphilic diblock copolymers PBnCL-*b*-PME₃PyCL, PCL-*b*-PME₃PyCL, and PCL-*b*-PME₃CL.

Fig. S18. Turbidity curves of homopolymer PME₃PyCL in water.

Table S1. LCST values of homopolymer PME₃PyCL in water.

Fig. S19. Turbidity curves of homopolymer PME₃PyCL in PBS ($\times 1$, pH = 7.4).

Table S2. LCST values of homopolymer PME₃PyCL in PBS.

Fig. S20. CMC plot of homopolymer PME₃PyCL in PBS ($1\times$, pH = 7.4) determined using pyrene as a fluorescence probe.

Fig. S21. Turbidity curves of amphiphilic diblock copolymers PBnCL-*b*-PME₃PyCL, PCL-*b*-PME₃PyCL, and PCL-*b*-PME₃CL (1 mg/mL) in PBS ($\times 1$, pH = 7.4).

Table S3. LCST values of amphiphilic diblock copolymers PBnCL-*b*-PME₃PyCL, PCL-*b*-PME₃PyCL, and PCL-*b*-PME₃CL in PBS ($1\times$, pH = 7.4) (polymer concentration = 1 mg/mL).

Fig. S22. DLS of Que-loaded micelle solutions obtained by dialysis method in PBS ($1\times$, pH = 7.4).

Fig. S23. Calibration curve of Que in DMSO : DI water (1 : 1).

1. MATERIALS AND METHODS

1.1 Materials

All commercially available chemicals were obtained from Sigma-Aldrich or Fisher Scientific. Prior to use, benzyl alcohol (BnOH) and ϵ -caprolactone were purified by vacuum distillation. Phosphate buffer saline (1 \times , pH = 7.4, NaCl 137 mM, KCl 2.7 mM, and 11.9 mM phosphates) was prepared by dilution of phosphate buffer saline (10 \times) solution with Milli-Q water. All glassware used for polymerizations was kept in an oven heated at 120 °C for 24 h and allowed to cool down in a desiccator before use. All polymerizations were performed under nitrogen.

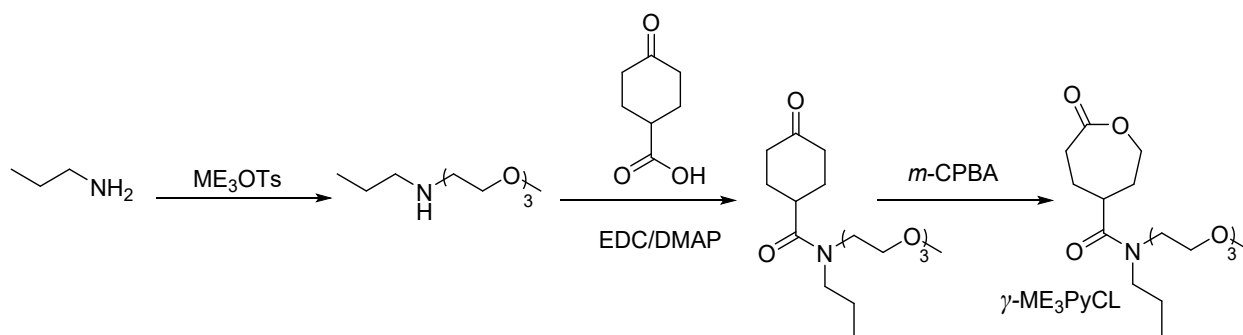
1.2 Analysis

A Bruker AVANCE III (500 MHz) nuclear magnetic resonance (NMR) instrument was used to collect ^1H spectra using CDCl_3 as the solvent. Matrix-assisted laser desorption/ionization time-of-flight (MALDI-ToF) mass spectrum was acquired using a Shimadzu AXIMA Confidence MALDI-TOF Mass Spectrometry in reflection mode with dithranol matrix and sodium trifluoromethanesulfonate salt. Size exclusion chromatography (SEC) measurements were obtained using a Shimadzu HPLC instrument equipped with an Agilent column connected to the Shimadzu refractive index detector with N,N-dimethylformamide (DMF) as eluent, and poly(methyl methacrylate) (PMMA) standard calibration. Differential scanning calorimetry (DSC) was performed on a TA Instruments Q100 DSC under nitrogen. A temperature-controlled Cary5000 UV-vis spectrometer was used for the turbidimetric assay of the synthesized polymers. A 0.5 °C min $^{-1}$ heating rate was applied to a quartz cuvette with a path length of 1.0 cm. Fluorescence spectroscopy of the samples was performed using a PerkinElmer LS 50 BL luminescence spectrometer. The size and distribution of the particles were measured through dynamic light scattering (DLS) using a Malvern Zetasizer Nano ZS instrument equipped with a

He-Ne laser (633 nm) and 173° backscatter detector. Using the same sample and the same DLS instrument, zeta potential measurement was carried out in a capillary cell in an automatic mode. Transmission electron microscopy (TEM) analysis was conducted using a JEM-1400+ TEM (JEOL USA Inc., MA) with 2% phosphotungstic acid stain.

1.3 Synthesis of Monomers

The monomers γ -2-[2-(2-methoxyethoxy)ethoxy]ethoxy- ϵ -caprolactone (γ -ME₃CL) and γ -benzyloxy- ϵ -caprolactone (γ -BnCL) were synthesized following the reported procedure in literature.^{1, 2} The new difunctionalized γ -amide ϵ -CL monomer bearing a hydrophilic 2-[2-(2-methoxyethoxy)ethoxy]ethoxy (ME₃) group and a hydrophobic propyl (Py) group (γ -ME₃PyCL) was synthesized following a three-step reaction (Scheme S1).



Scheme S1. Synthesis of difunctionalized γ -amide ϵ -CL monomer γ -ME₃PyCL.

Procedure for the synthesis of N-(2-(2-(2-methoxyethoxy)ethoxy)ethyl)propan-1-amine

Methoxytriethylene glycol tosylate, ME₃OTs (9.0 g, 2.8 mmol), which was synthesized following a previously published procedure,³ and propylamine (13.3 g, 22.5 mmol) were added into a flask, and the mixture was stirred at 50 °C overnight. The reaction mixture was allowed to cool to room temperature, followed by adding NaOH (2.3 g, 5.7 mmol). The mixture was then stirred at 50 °C overnight, filtered, and evaporated *in vacuo*. The crude product was stirred with K₂CO₃, then re-filtered to obtain the pure product (5.0 g, 86% yield). ¹H NMR (500 MHz, CDCl₃) δ : 0.85-0.88 (t,

3H), 1.42-1.51 (m, 2H), 1.84 (s, 1H), 2.51-2.54 (t, 2H), 2.72-2.75 (t, 2H), 3.33 (s, 3H), 3.49-3.58 (m, 10H). ¹³C NMR (500 MHz, CDCl₃) δ: 11.74, 23.14, 49.22, 51.81, 58.99, 70.28, 70.48, 70.52, 70.56, 71.91.

Procedure for the synthesis of N-propyl-N-(2-(2-(2-methoxyethoxy)ethoxy)ethyl)-4-oxocyclohexane-1-carboxamide

4-Oxocyclohexane-1-carboxylic acid (3.8 g, 26.8 mmol), which was synthesized following reported procedures,⁴ *N*-(2-(2-(2-methoxyethoxy)ethoxy)ethyl)dodecan-1-amine) (5.0 g, 24.4 mmol), 4-(dimethylamino)pyridine (DMAP) (1.5 g, 12.2 mmol), and dichloromethane were cooled to 0 °C in a round-bottom flask. A solution of 1-ethyl-3-(3-dimethylamino)-propylcarbodiimide hydrochloride (EDCI) (6.1 g, 31.7 mmol) in DCM was added dropwise to the cooled solution. The reaction was stirred overnight, followed by evaporating the solvent *in vacuo*, then extraction with ethyl acetate. The product was isolated by chromatography using ethyl acetate (4.0 g, 50% yield). ¹H NMR (500 MHz, CDCl₃) δ: 0.88-0.98 (tt, 3H), 1.52-1.70 (m, 2H), 2.02-2.11 (m, 4H), 2.33-2.40 (m, 2H), 2.51-2.59 (m, 2H), 2.88-2.93/3.10-3.16 (m, 1H), 3.33-3.40 (m, 5H), 3.54-3.65 (m, 12H). ¹³C NMR (500 MHz, CDCl₃) δ: 11.22, 11.26, 20.90, 22.78, 29.18, 37.84, 38.06, 40.01, 40.07, 46.10, 47.53, 47.71, 50.85, 59.05, 69.34, 69.42, 70.41, 70.52, 70.57, 70.64, 70.73, 70.88, 71.91, 71.95, 174.33, 174.82, 210.16, 210.57.

Procedure for the synthesis of N-propyl-N-(2-(2-(2-methoxyethoxy)ethoxy)ethyl)-7-oxoheptane-4-carboxamide (γ-ME₃PyCL)

A solution of *N*-propyl-*N*-(2-(2-(2-methoxyethoxy)ethoxy)ethyl)-4-oxocyclohexane-1-carboxamide (2.2 g, 6.7 mmol) in dichloromethane was added to a solution of 77% m-chloroperoxybenzoic acid (2.53 g, 24.8 mmol) in dichloromethane at 0 °C. The reaction was stirred for 24 h then the solvent was evaporated *in vacuo*. The product was isolated by flash

chromatography using hexane/ethyl acetate (2.2 g, 96% yield). ^1H NMR (500 MHz, CDCl_3) δ : 0.85-0.93 (tt, 3H), 1.48-1.63 (m, 2H), 1.89-2.12 (m, 4H), 2.57-2.64 (m, 1H), 2.78-2.95/3.04-3.10 (m, 2H), 3.23-3.37 (m, 5H), 3.44-3.64 (m, 12H), 4.16-4.21 (m, 1H), 4.45-4.53 (m, 1H). ^{13}C NMR (500 MHz, CDCl_3) δ : 20.85, 22.79, 25.59, 25.63, 32.10, 32.15, 32.31, 32.41, 40.78, 40.81, 46.09, 47.61, 50.83, 59.04, 66.86, 67.09, 69.14, 69.32, 70.39, 70.50, 70.55, 70.60, 70.65, 70.78, 71.89, 71.94, 173.94, 174.57, 175.20, 175.53. MALDI-ToF: 369.09 [M^+Na^+].

1.4 Critical Micelle Concentration (CMC) Determination

Pyrene was used to determine the CMC of the polymers in phosphate buffer solution (PBS) at pH 7.4. Polymers of various concentrations from 1.0 mg mL^{-1} to $1.0 \times 10^{-7} \text{ mg mL}^{-1}$ and a constant amount of pyrene, both in THF, were added to PBS. The final concentration of pyrene in the solution was $3.0 \times 10^{-7} \text{ M}$. The mixture was stirred constantly until all the THF evaporated. The samples were subjected to fluorescence spectroscopy, and the CMC was considered as the concentration at which an abrupt change in the ratio of peak intensity at 338 nm to that at 334 nm (I_{338}/I_{334}) from the excitation spectra of pyrene versus $\log(c)$ plot.

1.5 Lower Critical Solution Temperature (LCST) Measurement

LCST values of polymers were determined by measuring the 50% drop in transmittance of polymer/PBS solutions using a thermo UV-vis spectrometer. For homopolymer PME_3PyCL and diblock copolymer $\text{PBnCL-}b\text{-PME}_3\text{PyCL}$, polymer aqueous solutions were prepared by directly dissolving polymer in PBS and equilibrating for 24 hrs. For diblock copolymers $\text{PCL-}b\text{-PME}_3\text{PyCL}$ and $\text{PCL-}b\text{-PME}_3\text{CL}$, polymer aqueous solutions were prepared by dialyzing a polymer/THF solution against PBS for 24 hrs because the polymers could not dissolve in PBS by direct dissolution.

1.6 Preparation of Empty Micelles

Empty micelles were prepared by self-assembly of amphiphilic diblock copolymers in PBS (1×, pH = 7.4) using dialysis method. First, 2.0 mg polymer was dissolved in 0.6 mL THF. Then the polymer/THF solution was added dropwise to 2.0 mL PBS (1×, pH = 7.4) with homogenization. The final polymer concentration in PBS (1×, pH = 7.4) was 1 mg/mL. After homogenizing for 10-15 min, the mixture was transferred to a dialysis bag (MW cutoff: 3500 Da) to dialyze against 500 mL PBS (1×, pH = 7.4) for 24 hrs. When dialysis was completed, the micelle solution was filtered with a 0.45 *um* nylon syringe filter.

1.7 Preparation of Quercetin Loaded Micelles

Quercetin-loaded micelles were prepared using the dialysis method with a polymer/drug ratio of 10:1. 2.0 mg Polymer in 0.3 mL THF and 0.2 mg Quercetin (Que) in 0.3 mL THF were mixed and then added to 2.0 mL PBS (1×, pH = 7.4) or DI water dropwise with homogenizing for 15 min. The mixture was then transferred to a dialysis bag (MW cutoff: 3500 Da) and dialyzed against 500 mL (1×, pH = 7.4) or DI water for 24 hrs to remove THF and unencapsulated Que. Que-loaded micelle solutions were obtained by filter using a 0.45 *um* nylon syringe filter. The Que-loaded micelles were collapsed by dilution of DMSO ($V_{\text{micelle solution}} : V_{\text{DMSO}} = 1:1$). The concentration of Que was determined by using a pre-plotted calibration curve of Que. Drug loading capacity (DLC) and drug loading efficiency (EE) were calculated using the equations below.

$$\text{DLC (wt\%)} = \frac{\text{mass of Que loaded}}{\text{total mass of polymer}} \times 100\% \quad (\text{Eq. 1})$$

$$\text{EE (wt\%)} = \frac{\text{mass of Que loaded}}{\text{total mass of Que}} \times 100\% \quad (\text{Eq. 2})$$

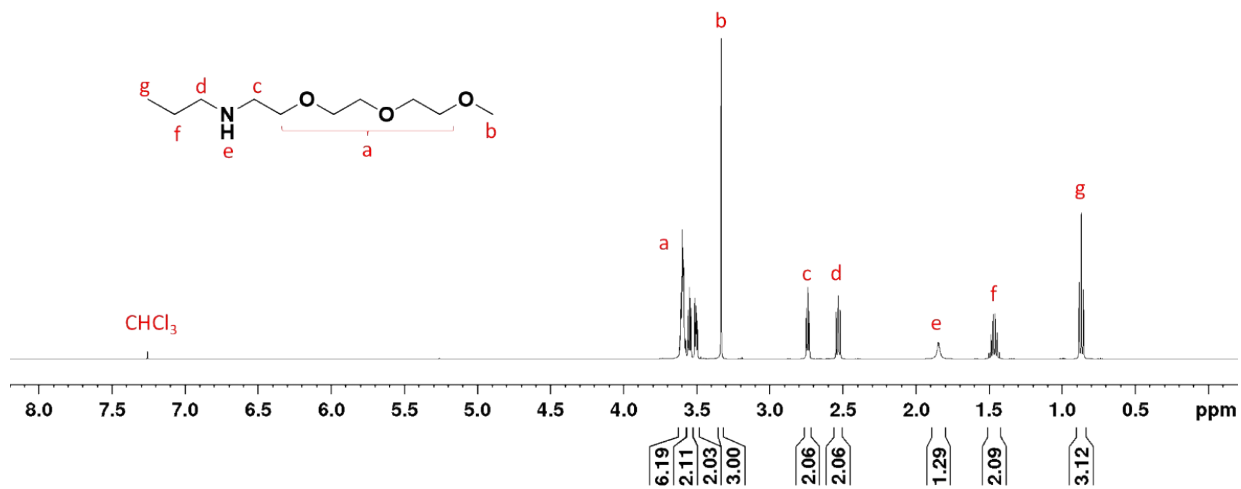


Fig. S1. ¹H NMR spectrum of the intermediate compound *N*-(2-(2-(2-methoxyethoxy)ethoxy)ethyl)propan-1-amine.

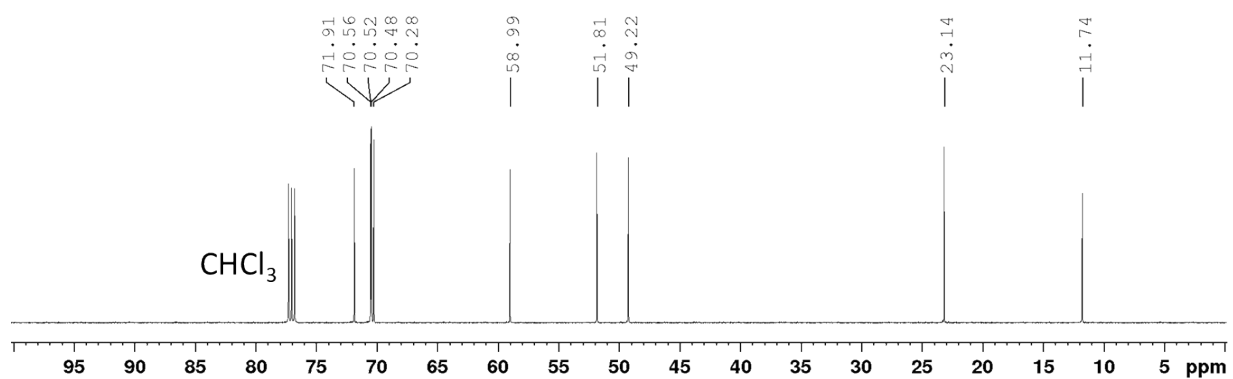


Fig. S2. ¹³C NMR spectrum of the intermediate compound *N*-(2-(2-(2-methoxyethoxy)ethoxy)ethyl)propan-1-amine.

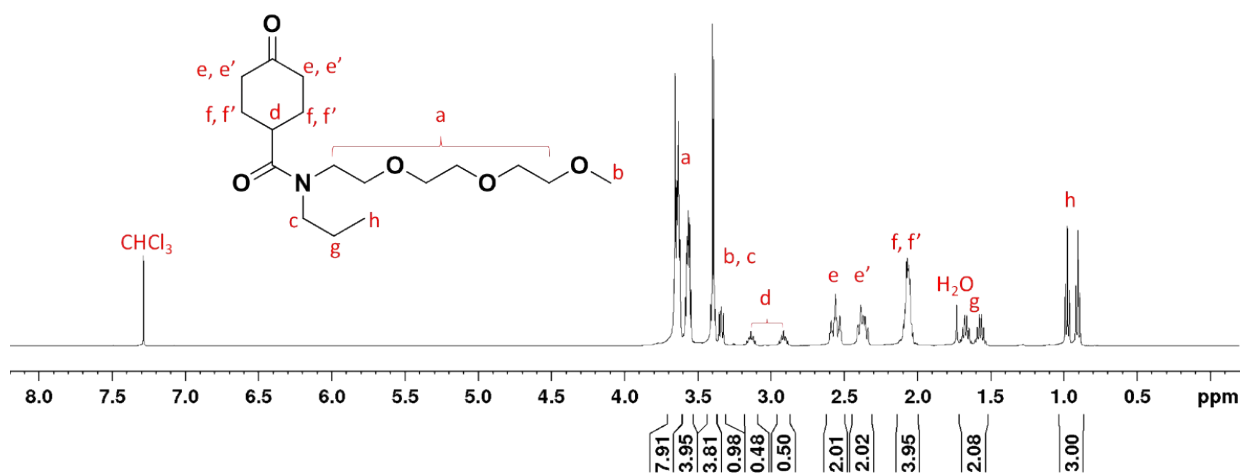


Fig. S3. ^1H NMR spectrum of the intermediate compound *N*-propyl-*N*-(2-(2-(2-methoxyethoxy)ethoxy)ethyl)-4-oxocyclohexane-1-carboxamide.

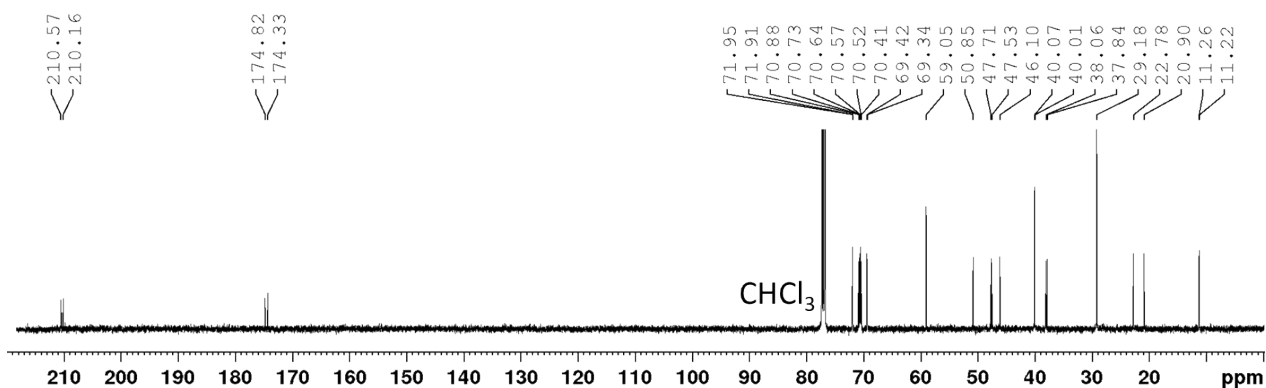


Fig. S4. ^{13}C NMR spectrum of the intermediate compound *N*-propyl-*N*-(2-(2-(2-methoxyethoxy)ethoxy)ethyl)-4-oxocyclohexane-1-carboxamide.

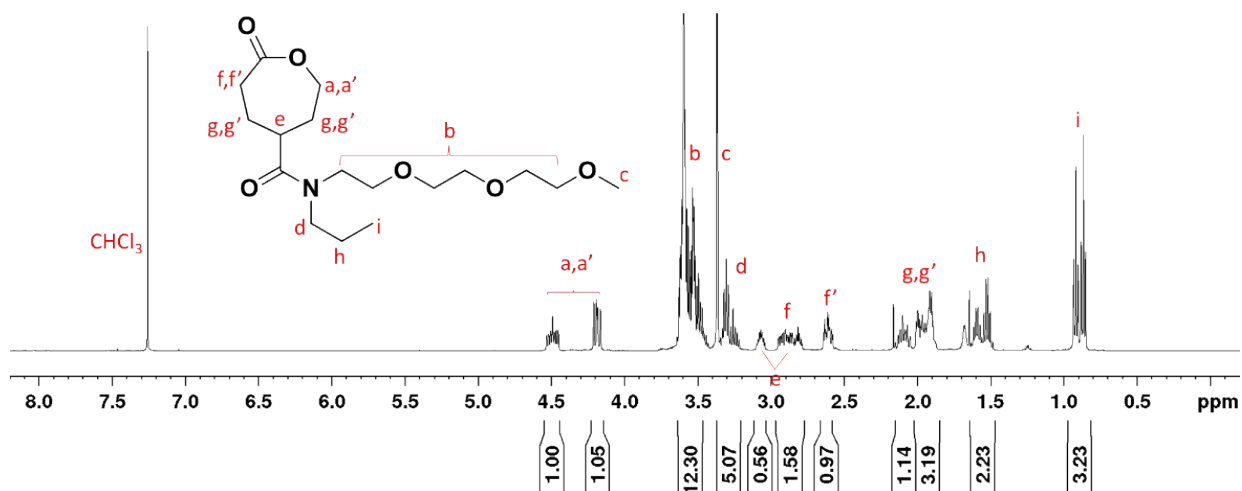


Fig. S5. ^1H NMR spectrum of monomer *N*-propyl-*N*-(2-(2-(2-methoxyethoxy)ethoxy)ethyl)-7-oxoxepane-4-carboxamide ($\gamma\text{-ME}_3\text{PyCL}$).

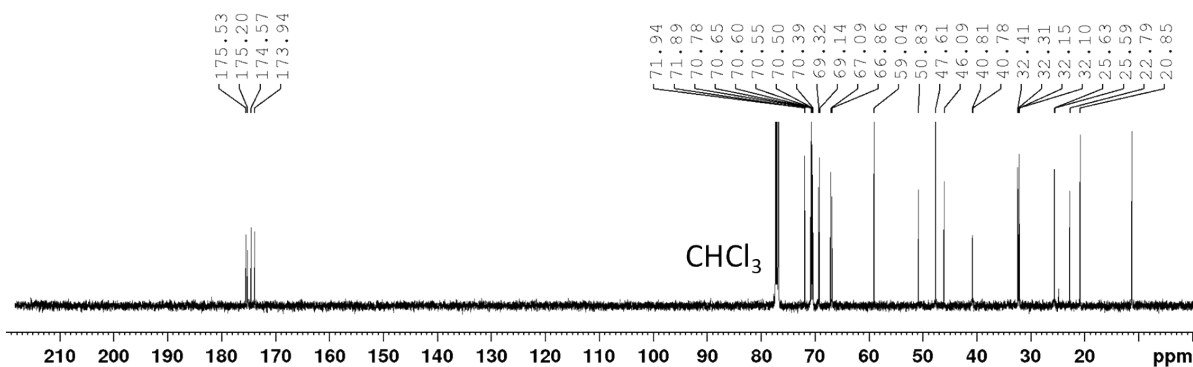


Fig. S6. ^{13}C NMR spectrum of monomer *N*-propyl-*N*-(2-(2-(2-methoxyethoxy)ethoxy)ethyl)-7-oxoxepane-4-carboxamide ($\gamma\text{-ME}_3\text{PyCL}$).

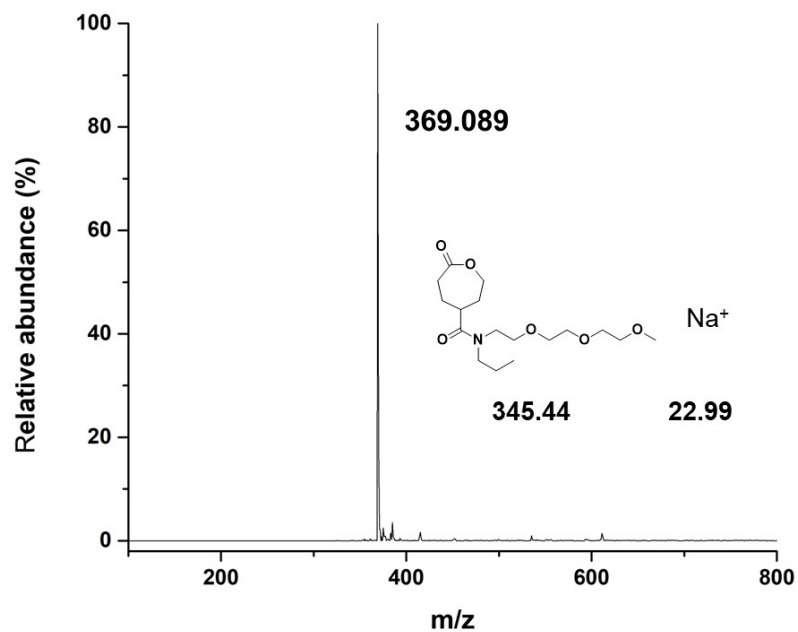


Fig. S7. MALDI-ToF mass spectrum of monomer *N*-propyl-*N*-(2-(2-(2-methoxyethoxy)ethoxy)ethyl)-7-oxoxepane-4-carboxamide (γ -ME₃PyCL).

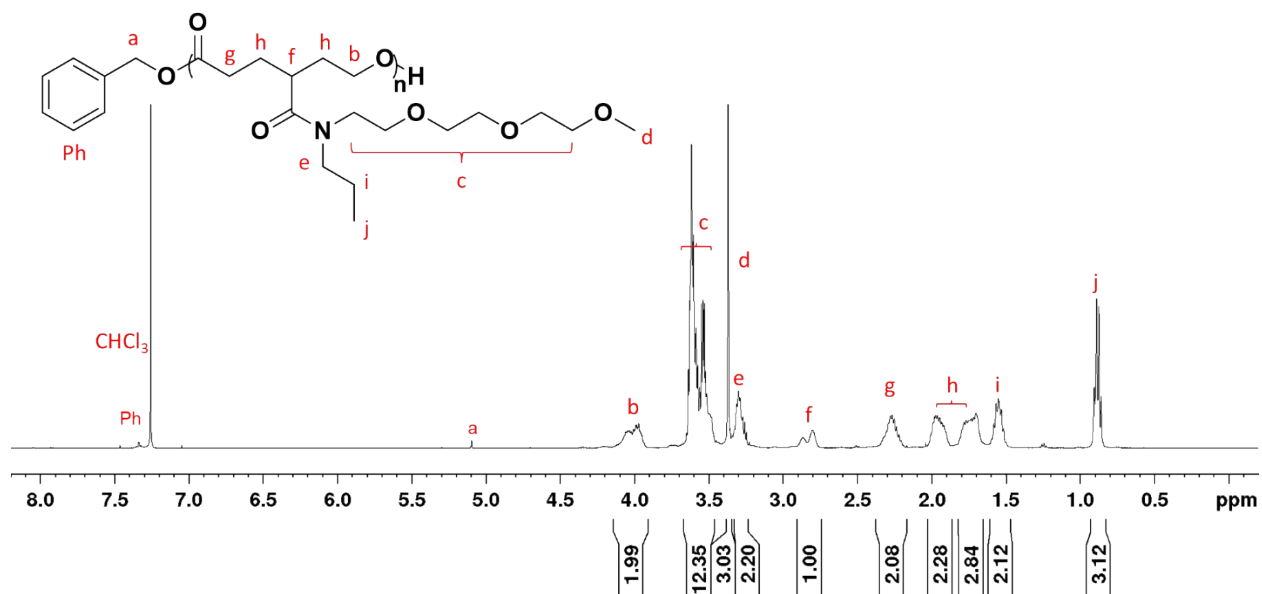


Fig. S8. ¹H NMR spectrum of the homopolymer poly(*N*-propyl-*N*-(2-(2-(2-methoxyethoxy)ethoxy)ethyl)-7-oxoxepane-4-carboxamide) PME₃PyCL.

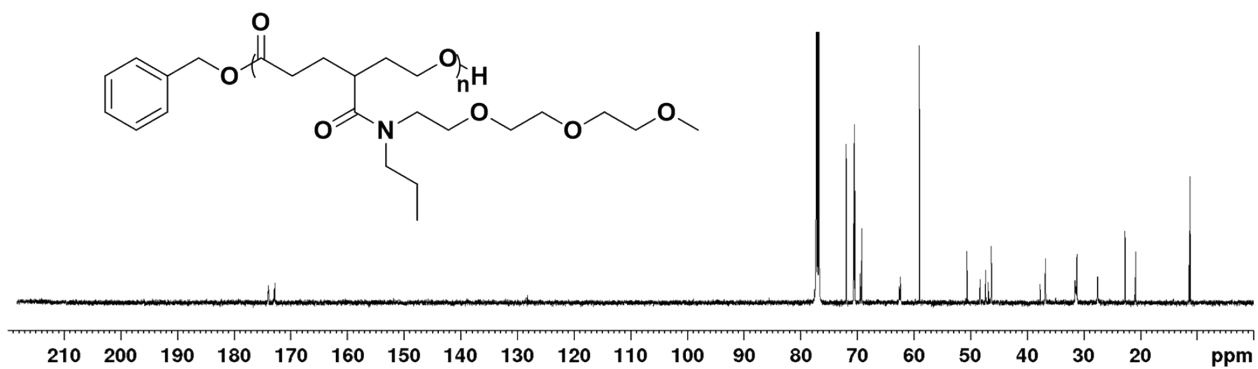


Fig. S9. ^{13}C NMR spectrum of the homopolymer poly(*N*-propyl-*N*-(2-(2-(2-methoxyethoxy)ethoxy)ethyl)-7-oxoheptan-4-carboxamide) PME_3PyCL .

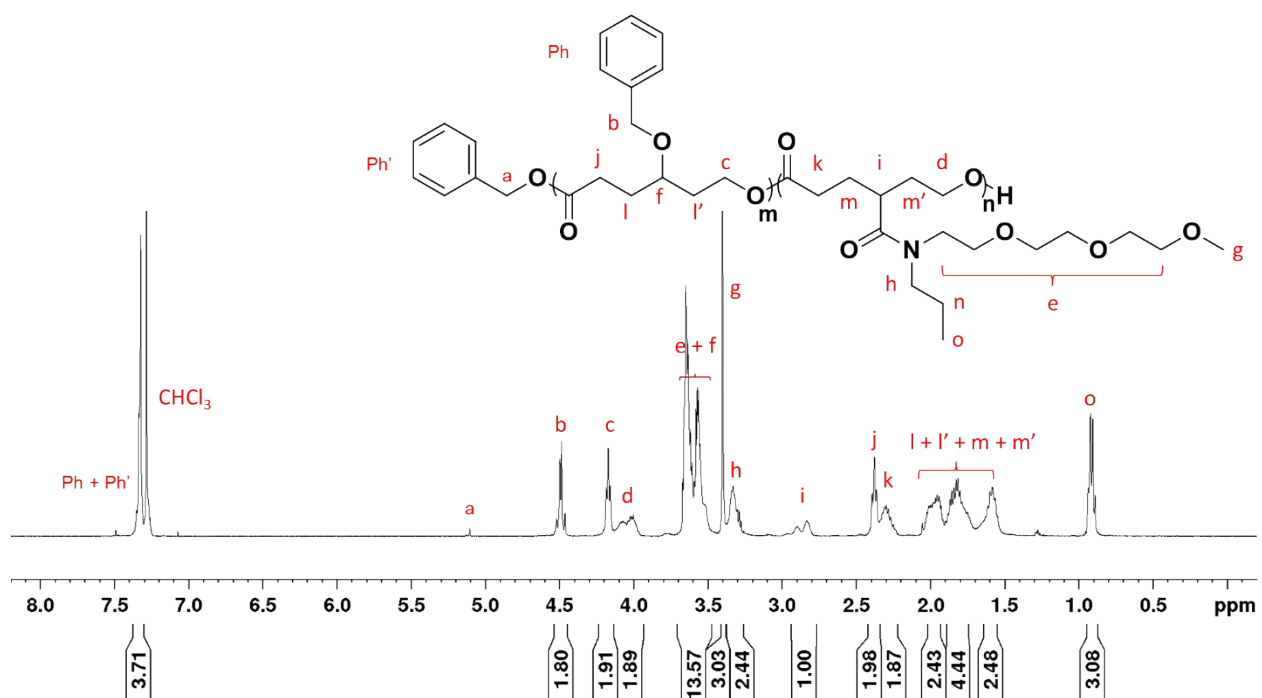


Fig. S10. ^1H NMR spectrum of the amphiphilic diblock copolymer poly(γ -benzyloxy- ϵ -caprolactone)-*b*-poly(*N*-propyl-*N*-(2-(2-(2-methoxyethoxy)ethoxy)ethyl)-7-oxoheptan-4-carboxamide) (PBnCL-*b*- PME_3PyCL).

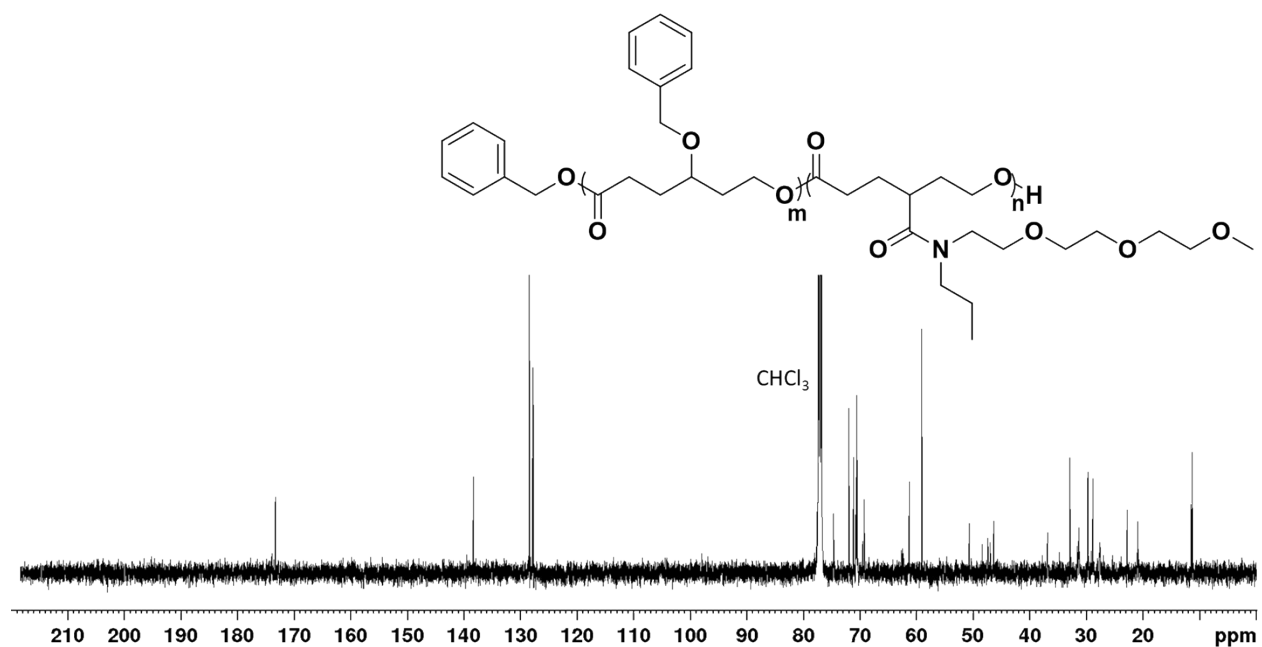


Fig. S11. ^{13}C NMR spectrum of the amphiphilic diblock copolymer poly(γ -benzyloxy- ϵ -caprolactone)-*b*-poly(*N*-propyl-*N*-(2-(2-(2-methoxyethoxy)ethoxy)ethyl)-7-oxoxepane-4-carboxamide) (PBnCL-*b*-PME₃PyCL).

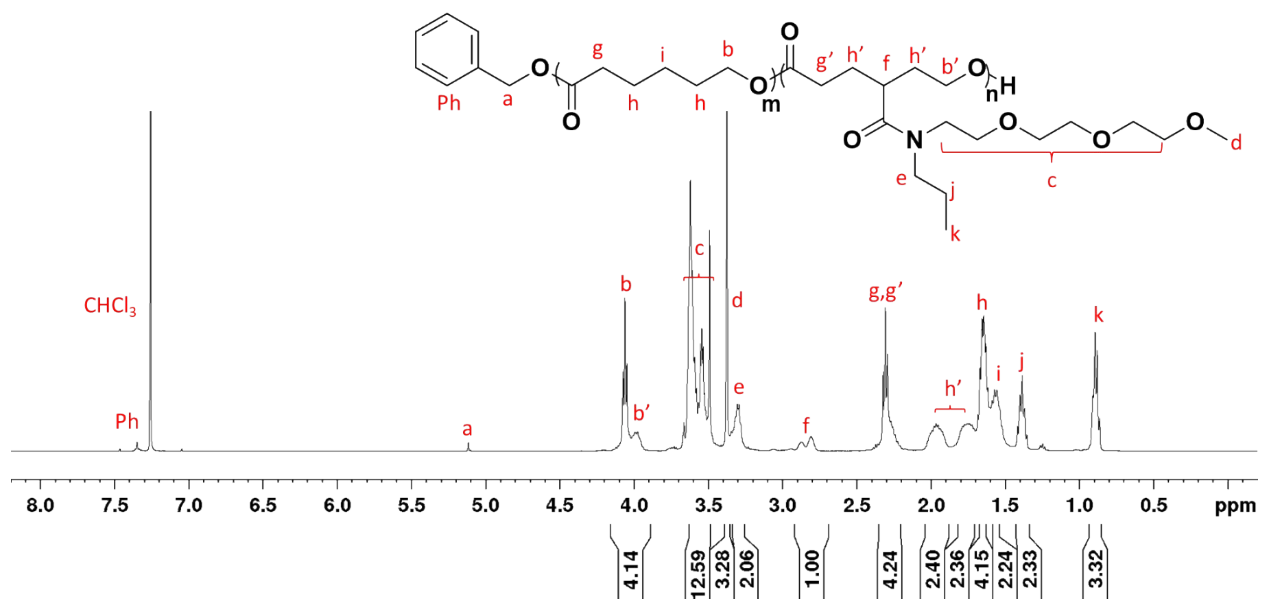


Fig. S12. ^1H NMR spectrum of the amphiphilic diblock copolymer polycaprolactone-*b*-poly(*N*-propyl-*N*-(2-(2-(2-methoxyethoxy)ethoxy)ethyl)-7-oxoxepane-4-carboxamide) (PCL-*b*-PME₃PyCL).

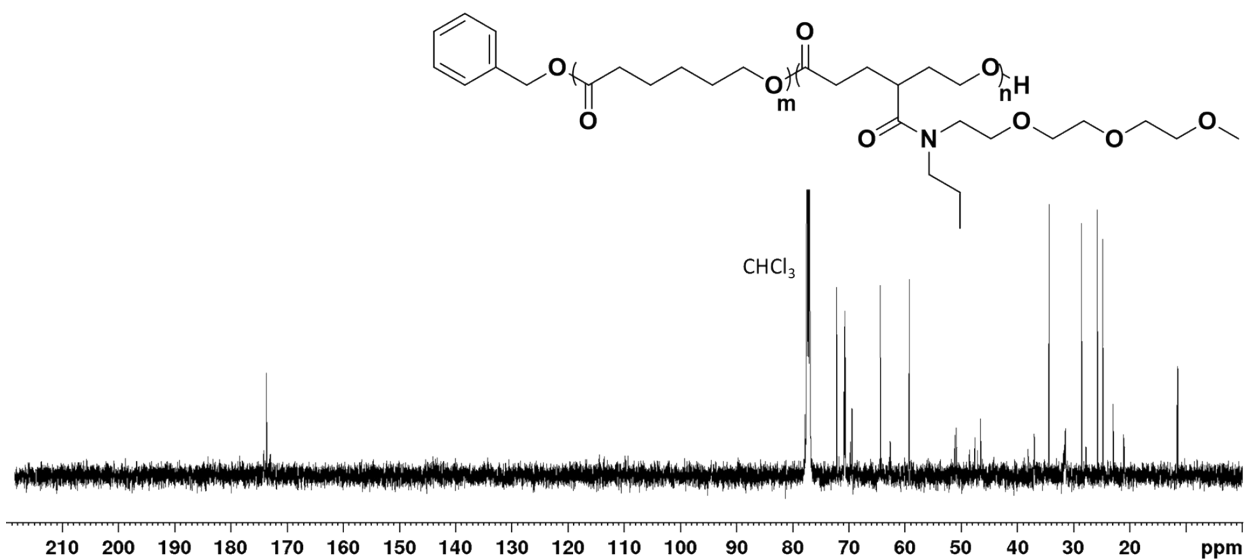


Fig. S13. ^{13}C NMR spectrum of the amphiphilic diblock copolymer polycaprolactone-*b*-poly(*N*-propyl-*N*-(2-(2-(2-methoxyethoxy)ethoxy)ethyl)-7-oxoxepane-4-carboxamide) (PCL-*b*-PME₃PyCL).

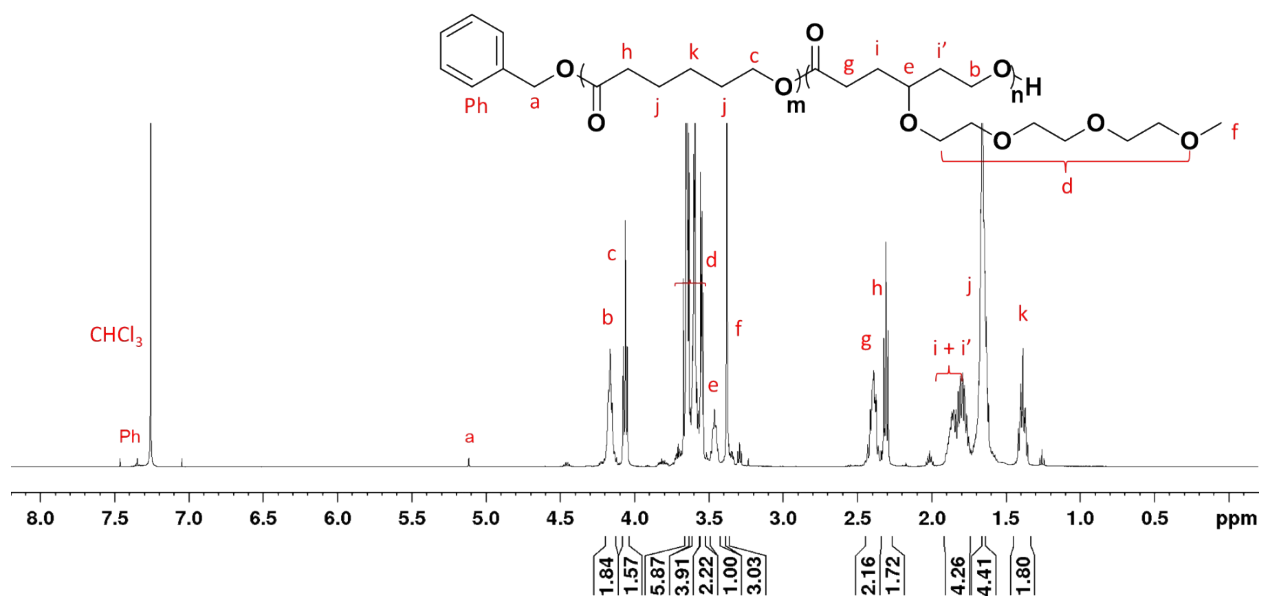


Fig. S14. ^1H NMR spectrum of the amphiphilic diblock copolymer polycaprolactone-*b*-poly(γ -2-(2-(2-methoxyethoxy)ethoxy)ethoxy- ϵ -caprolactone) (PCL-*b*-PME₃CL).

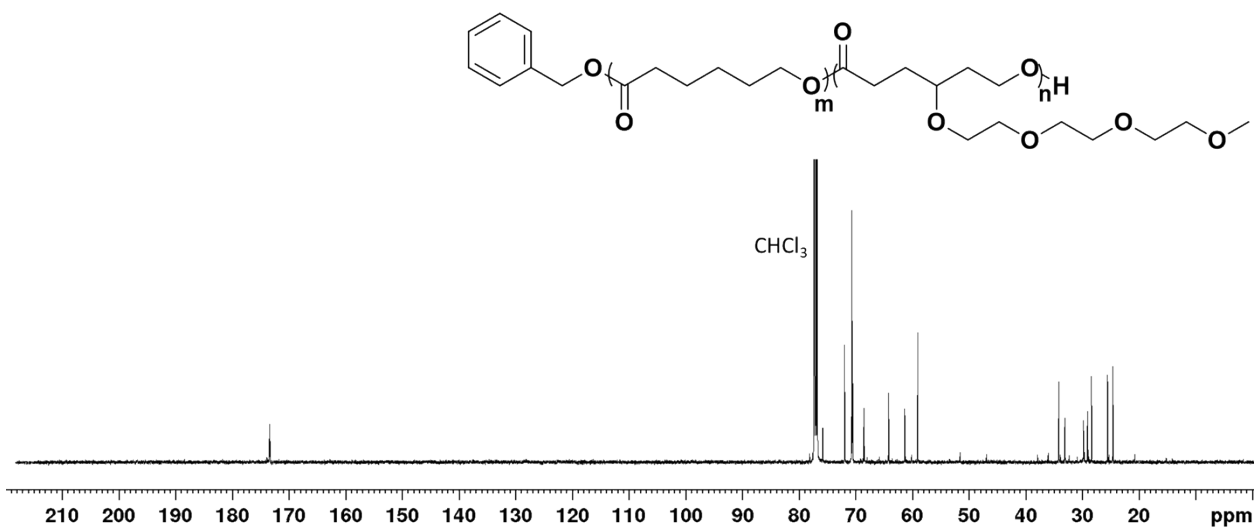


Fig. S15. ^{13}C NMR spectrum of the amphiphilic diblock copolymer polycaprolactone-*b*-poly(γ -2-(2-(2-methoxyethoxy)ethoxy)ethoxy- ϵ -caprolactone) (PCL-*b*-PME₃CL).

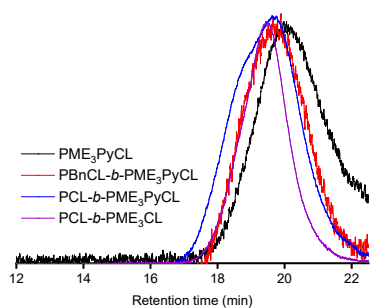


Fig. S16. Size exclusion chromatography of homopolymer PME₃PyCL and amphiphilic diblock copolymers PBnCL-*b*-PME₃PyCL, PCL-*b*-PME₃PyCL, and PCL-*b*-PME₃CL.

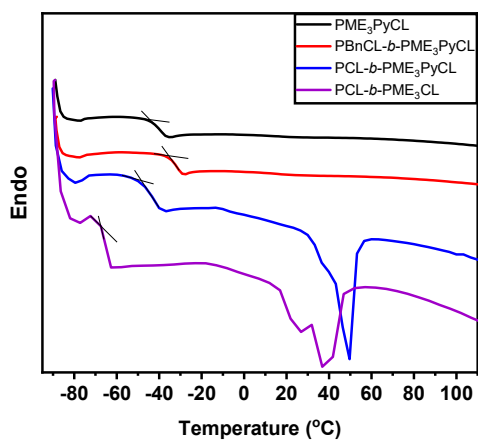


Fig. S17. Glass transition temperature of homopolymer PME₃PyCL and amphiphilic diblock copolymers PBnCL-*b*-PME₃PyCL, PCL-*b*-PME₃PyCL, and PCL-*b*-PME₃CL.

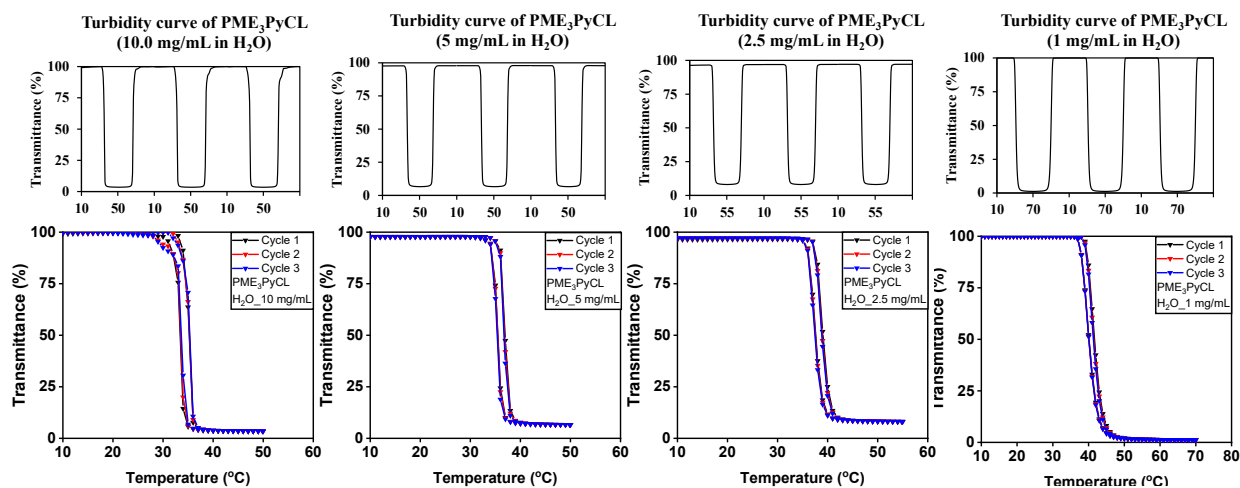


Fig. S18. Turbidity curves of homopolymer PME₃PyCL in water.

Table S1. LCST values of homopolymer PME₃PyCL in water.

Polymer concentration in water (mg/mL)	LCST (°C) ^a							
	Cycle 1		Cycle 2		Cycle 3		Mean ± SD	
	Heating	Cooling	Heating	Cooling	Heating	Cooling	Heating (n = 3)	Cooling (n = 3)
10	35.3	33.5	35.3	33.5	35.4	33.7	35.3 ± 0.1	33.6 ± 0.1
5	37.0	35.5	36.9	35.5	36.8	35.4	36.9 ± 0.1	35.5 ± 0.1
2.5	39.1	37.7	39.0	37.6	38.9	37.5	39.0 ± 0.1	37.6 ± 0.1
1	41.7	40.2	41.5	40.1	41.4	40.1	41.5 ± 0.1	40.1 ± 0.1

^a Determined from thermo UV-Vis spectroscopy

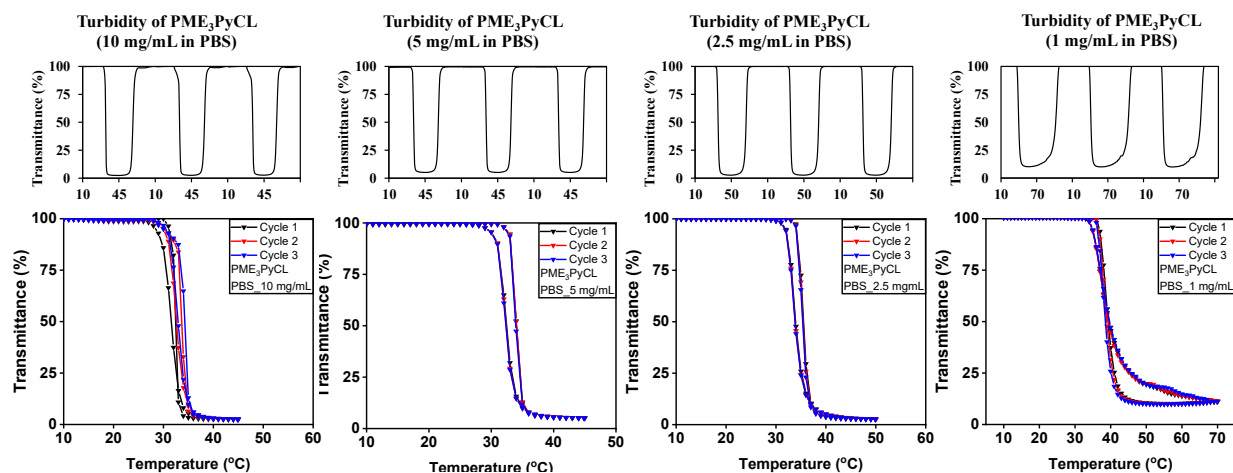


Fig. S19. Turbidity curves of homopolymer PME_3PyCL in PBS ($\times 1$, $\text{pH} = 7.4$).

Table S2. LCST values of homopolymer PME_3PyCL in PBS ($1\times$, $\text{pH} = 7.4$).

Polymer concentration in PBS ^b (mg/mL)	LCST ($^{\circ}\text{C}$) ^a							
	Cycle 1		Cycle 2		Cycle 3		Mean \pm SD	
	Heating	Cooling	Heating	Cooling	Heating	Cooling	Heating (n = 3)	Cooling (n = 3)
10	32.5	31.6	33.7	32.6	34.3	32.9	33.5 \pm 0.9	32.4 \pm 0.7
5	34.1	32.5	34.1	32.4	34.0	32.4	34.1 \pm 0.1	32.4 \pm 0.1
2.5	35.6	34.0	35.5	33.9	35.4	33.9	35.5 \pm 0.1	33.9 \pm 0.1
1	39.6	39.6	39.0	39.5	38.6	39.6	39.1 \pm 0.1	39.6 \pm 0.1

^a Determined from thermo UV-Vis spectroscopy.

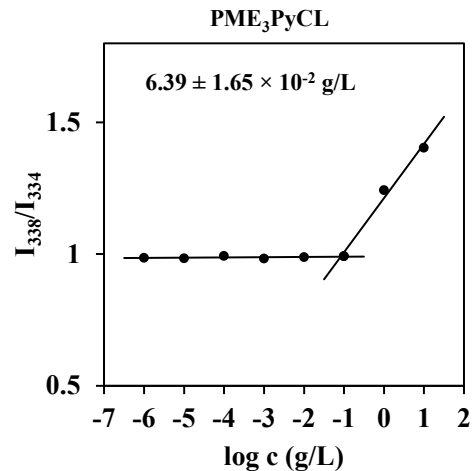


Fig. S20. CMC plot of homopolymer PME₃PyCL in PBS (1×, pH = 7.4) determined using pyrene as a fluorescence probe.

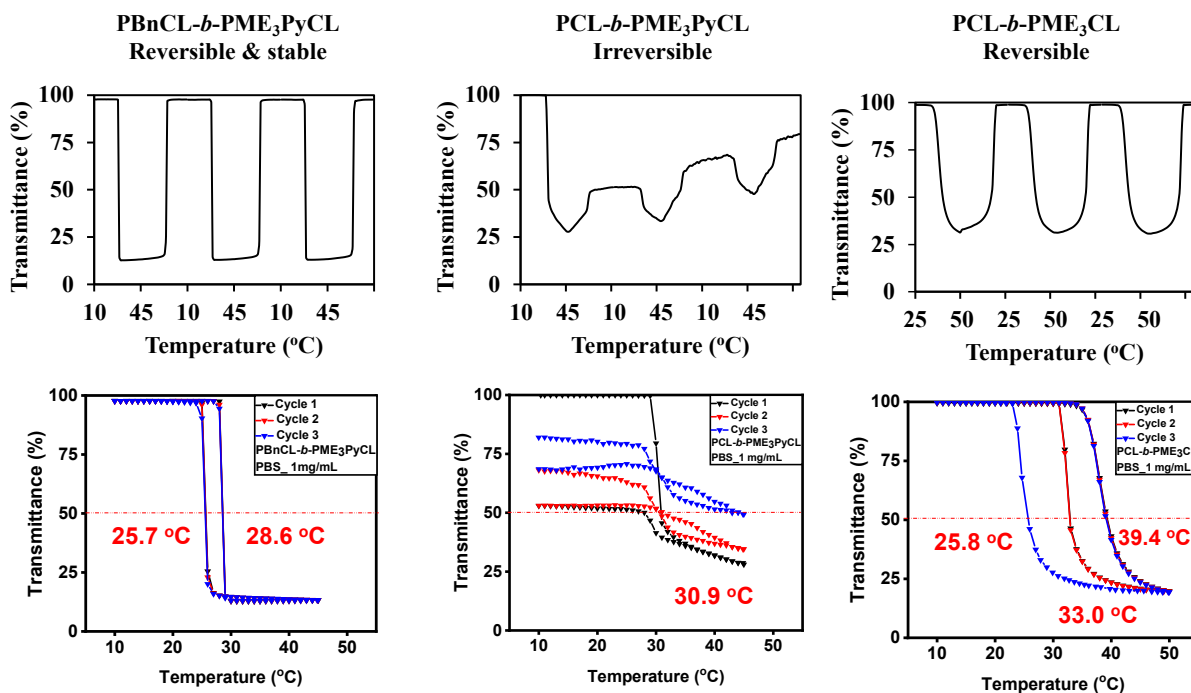


Fig. S21. Turbidity curves of amphiphilic diblock copolymers PBnCL-*b*-PME₃PyCL, PCL-*b*-PME₃PyCL, and PCL-*b*-PME₃CL (1 mg/mL) in PBS (×1, pH = 7.4).

Table S3. LCST values of amphiphilic diblock copolymers PBnCL-*b*-PME₃PyCL, PCL-*b*-PME₃PyCL, and PCL-*b*-PME₃CL in PBS (1×, pH = 7.4) (polymer concentration = 1 mg/mL).

Polymer	LCST (°C) ^a							
	Cycle 1		Cycle 2		Cycle 3		Mean ± SD	
	Heating	Cooling	Heating	Cooling	Heating	Cooling	Heating (n = 3)	Cooling (n = 3)
PBnCL- <i>b</i> -PME ₃ PyCL	28.6	25.7	28.6	25.7	28.6	25.7	28.6 ± 0.0	25.7 ± 0.0
PCL- <i>b</i> -PME ₃ PyCL	30.9	NA	NA	NA	NA	NA	NA	NA
PCL- <i>b</i> -PME ₃ CL	39.4	33.0	39.4	33.0	39.4	25.8	39.4 ± 0.0	30.6 ± 4.6

^a Determined from thermo UV-Vis spectroscopy (n = 3).

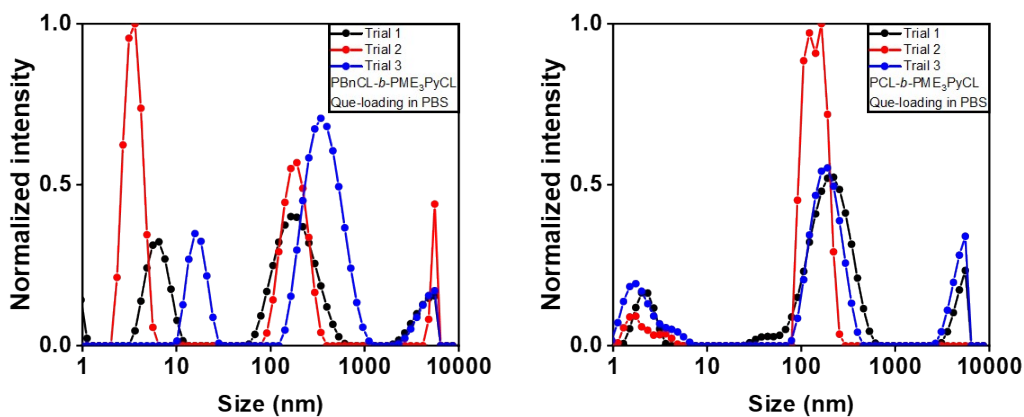


Fig. S22. DLS of Que-loaded micelle solutions obtained by dialysis in PBS (1×, pH = 7.4).

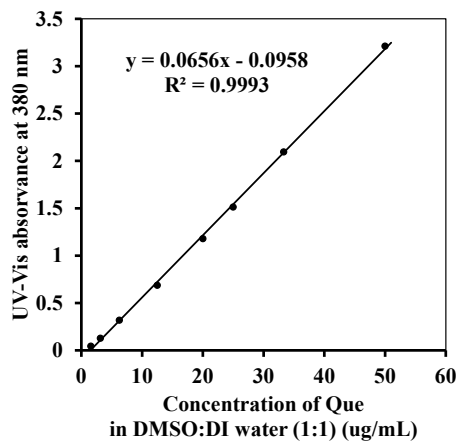


Fig. S23. Calibration curve of Que in DMSO : DI water (1 : 1).

1. Soltantabar, P.; Calubaquib, E. L.; Mostafavi, E.; Biewer, M. C.; Stefan, M. C., Enhancement of loading efficiency by coloaded of doxorubicin and quercetin in thermoresponsive polymeric micelles. *Biomacromolecules* **2020**, *21*, 1427-1436.
2. Hao, J.; Cheng, Y.; Ranatunga, R. U.; Senevirathne, S.; Biewer, M. C.; Nielsen, S. O.; Wang, Q.; Stefan, M. C., A combined experimental and computational study of the substituent effect on micellar behavior of γ -substituted thermoresponsive amphiphilic poly (ϵ -caprolactone) s. *Macromolecules* **2013**, *46*, 4829-4838.
3. Hao, J.; Servello, J.; Sista, P.; Biewer, M. C.; Stefan, M. C., Temperature-sensitive aliphatic polyesters: synthesis and characterization of γ -substituted caprolactone monomers and polymers. *Journal of Materials Chemistry* **2011**, *21*, 10623-10628.
4. Wen, L.; Zhang, S.; Xiao, Y.; He, J.; Zhu, S.; Zhang, J.; Wu, Z.; Lang, M., Organocatalytic ring-opening polymerization toward poly (γ -amide- ϵ -caprolactone) s with tunable lower critical solution temperatures. *Macromolecules* **2020**, *53*, 5096-5104.